NANO LETTERS

2006
Vol. 6, No. 2
313−317

Structure of Semidilute Single-Wall Carbon Nanotube Suspensions and Gels

L. A. Hough,*,†,‖ M. F. Islam,*,†,⊥ B. Hammouda,‡ A. G. Yodh,† and P. A. Heiney†

Department of Physics and Astronomy, University of Pennsylvania, 209 South 33rd Street, Philadelphia, Pennsylvania 19104-6396, and National Institute of Standards and Technology, Gaithersburg, Maryland 20899

Received September 19, 2005; Revised Manuscript Received December 7, 2005

ABSTRACT

The microscopic network structure of surfactant-stabilized single-wall carbon nanotubes (SWNTs) in water was investigated as a function of SWNT concentration in the semidilute (overlapping) regime using small-angle neutron scattering (SANS). Most of the samples exhibit rigid rod behavior (i.e., Q^{-1} intensity variation) at large scattering wavevector, Q, and a crossover to network behavior (i.e., $\sim Q^{-2}$ intensity variation) at low Q. The mesh size, ξ, of the network was determined from the crossover of rigid rod to network behavior in the SANS intensity profile and was found to decrease with increasing SWNT concentration. When the dispersion quality of these associating rigid rods was degraded, only $\sim Q^{-2}$ intensity variation was observed at both high and low Q. Small-angle X-ray scattering measurements of the same stable dispersions were relatively insensitive to network structure because of poor contrast between SWNTs and surfactant.

Many potential applications[1−9] of the unique physical properties of single-wall carbon nanotubes (SWNTs) employ these novel macromolecules at semidilute concentrations. Since individual SWNTs are stiff,[10] possessing a persistence length roughly 100 times the average SWNT length of ∼200 nm,[11,12] semidilute suspensions of SWNTs are essentially cross-linked rigid rod networks whose cross-link density depends on SWNT volume fraction. Measurement of the microscopic structure of these materials is of potential importance for nanotube materials processing and for investigation of the relationship between the microscopic structure and macroscopic viscoelastic[12−14] properties of rigid rod networks. To date, however, the microscopic structure of *semidilute* SWNT suspensions remains largely unexplored.

Thus far, a few experimental investigations of the microscopic structure of SWNT suspensions have been carried out in the *dilute* regime (i.e., SWNT concentration ≤0.1 wt%), using various scattering techniques.[15−21] SWNTs are rigid rods, and although the scattering intensity of isolated rigid rods is expected to exhibit a Q^{-1} variation, recent scattering measurements in the dilute regime have sometimes been contradictory, presumably due to dispersion quality.[15−21] For example, scattering from poorly dispersed SWNT suspensions containing branched, ropelike SWNT bundles exhibited Q^{-2} intensity variation[15−19] and appeared flexible in cryo-TEM (transmission electron microscopy) images.[22] On the other hand, stable SWNT dispersions containing isolated nanotubes have shown the expected Q^{-1} intensity variations,[15−17,20,21] and appeared straight in cryo-TEM images.[22]

In this paper, we report small-angle neutron scattering (SANS) measurements of the microscopic network structure of SWNT suspensions and gels in the *semidilute* regime. The samples were aqueous suspensions of sodium dodecylbenzenesulfonate (NaDDBS) stabilized SWNTs.[11] The SWNT suspensions exhibit a rigidity percolation transition with an onset of solidlike elasticity at a volume fraction of $\phi = 0.3$ wt%.[12] At SWNT concentrations below rigidity percolation, the suspensions flow freely under the influence of gravity (see Figure 1a). At higher concentrations, the suspensions form elastic networks (gels), presumably due to bond formation between the SWNTs at overlapping contact points (see parts b and c of Figure 1).[12,23] Such elastic networks might be expected to consist of overlapping isolated SWNTs with a mesh size, ξ, corresponding to the average distance between contacts, as illustrated in Figure 1d. Rheological experiments suggest that ξ decreases with increasing SWNT concentration,[12] but direct measurements of the dependence of ξ on SWNT concentration have not been reported. Ideally the scattering from such networks of stiff rods should exhibit a SANS intensity profile of Q^{-1} for $2\pi/\xi < Q < 2\pi/D$ (D is the rod diameter), and $\sim Q^{-2}$ for $Q < 2\pi/\xi$, as illustrated in Figure 1e.[24] Indeed, SANS measurements of dilute suspen-

* Corresponding authors: E-mail: larry.hough@us.rhodia.com, mohammad@andrew.cmu.edu.
† University of Pennsylvania.
‡ National Institute of Standards and Technology.
‖ Present address: Rhodia INC, 350 George Patterson Blvd., Bristol, PA 19007.
⊥ Present address: Department of Chemical Engineering and Department of Materials Science & Engineering, Carnegie Mellon University, Pittsburgh, PA 15213-3890.

10.1021/nl051871f CCC: $33.50 © 2006 American Chemical Society
Published on Web 01/26/2006

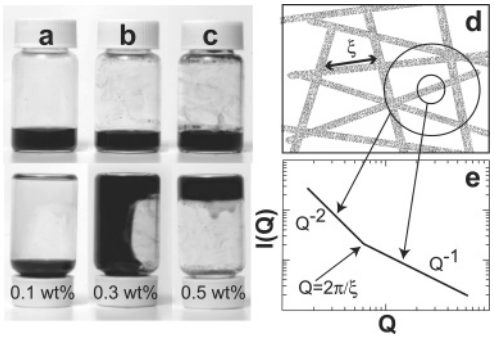

Figure 1. Photographs of SWNT suspensions. The ratio of SWNTs to NaDDBS is 1:5 by weight. (a) A 0.1 wt% SWNT suspension. The suspension freely flows under the influence of gravity when the bottle is turned upside down. (b) A 0.3 wt% SWNT suspension. (c) A 0.5 wt% SWNT suspension. The suspension forms an elastic solid (gel) that supports its own weight when the bottle is turned upside down. (d) Proposed structure of a SWNT gel. The mesh size, ξ is the distance between the junctions of the associated rigid rod network. (e) The prototypical scattering profile for a solution of overlapping rigid rods.

sions of NaDDBS stabilized SWNTs below the onset of elasticity have provided some evidence for this model, suggesting that a loose network is formed even at low SWNT concentration (0.1 wt%).[17]

A careful analysis of the SANS data enables us to quantitatively ascertain and correct for the effects of instrumental resolution and background surfactant scattering. Our measurements demonstrate rigid rod behavior and a crossover to network behavior across dilute and *semidilute* SWNT concentrations. To quantify this crossover effect, we have determined the concentration dependence of ξ from the rigid rod to network crossover point in the SANS intensity profile. We find that ξ decreases with increasing SWNT concentration, and we compare the measured ξ to the mesh sizes predicted from polymer theory.[25,26] We also compare SANS profiles of stable dispersions (with SWNT:NaDDBS ratio of 1:5) to profiles obtained from a suspension with surfactant concentration insufficient for prevention of SWNT aggregation (with 1:2 ratio[11]). In the latter measurements the rigid rod scattering signature and ergo the rigid rod to network crossover are absent. Finally, we show that X-ray scattering measurements of the same stable dispersions are relatively insensitive to network structure because of poor contrast between SWNTs and surfactant.

SWNTs were obtained in raw form from Carbon Nanotechnologies Inc. (HiPCO). The SWNT sample was purified according to previously described procedures.[9,27,28] After purification the material contains >90% SWNTs, with ~5% residual catalyst particles. The nanotubes were determined by atomic force microscopy to have an average diameter $D = 1.1 \pm 0.2$ nm and an average length $L = 165 \pm 80$ nm.[11] SANS samples were prepared by dispersing purified SWNTs in deuterium oxide (D_2O) with NaDDBS surfactant ($C_{12}H_{25}C_6H_4SO_3Na$) according to a previously described procedure.[11] The ratio of SWNTs to NaDDBS was 1:5 for all the samples unless otherwise noted. NaDDBS exists as isolated molecules or micelles in solution, or it is adsorbed onto the SWNTs. The ratio of free to bound NaDDBS generally will depend on SWNT and surfactant concentrations. The SANS samples were prepared in nitrogen to minimize the uptake of water, which causes incoherent background scattering. All SWNT suspensions were composed of 55−75% isolated tubes; the remainder contained small bundles with diameters less than 5 nm as measured by atomic force microscopy.[11]

For the SANS experiments, the samples were loaded into 2 mm quartz banjo cells. SANS data were collected at the 13 m NG3 line at the National Institute of Standards and Technology Center for Neutron Research. We achieved a large dynamic range in Q by combining the results from three different instrumental configurations: a 1 m SANS configuration, a 3 m SANS configuration, and a 13 m configuration with focusing lenses. The use of a contrast-matched H_2O/D_2O solvent would have simplified the data analysis but, unfortunately, also would have prohibitively increased the data collection time due to increased incoherent scattering.

SANS scattering profiles $I(Q)$ for several concentrations of SWNTs (0.1, 0.3, 0.5 wt%), stabilized by NaDDBS in D_2O are shown Figure 2. The scattering profiles for the corresponding surfactant alone (i.e., 0.5, 1.5, 2.5 wt% NaDDBS) in D_2O are also shown. The scattering peak at high Q in the NaDDBS samples is indicative of the presence of spherical surfactant micelles; in the SWNT-NaDDBS samples the peak might also contain contributions from surfactant hemimicelles coating the nanotubes.[11,29−31] The inset of each plot highlights the contribution of the rigid rod Q^{-1} and network $\sim Q^{-2}$ structure to the scattering profiles. The vertical line on each plot in the inset quantitatively indicates the crossover point Q_c.

Generally these measurements are complicated by surfactant contributions to the scattering intensity.[15−19,21] To describe the scattering data and quantitatively determine Q_c, we use a model that incorporates a crossover between isolated-rod and network behavior, a convolution with the instrumental resolution, a wide-angle component describing the surfactant contribution, and a constant incoherent contribution. The small-angle nanotube scattering was described with a simple sum of Q^{-2} and Q^{-1} power laws. To establish the wide-angle contribution of the surfactant to the scattered intensity, samples of pure NaDDBS were measured at the same concentration as those of the SWNT-NaDDBS samples, and the scattered line shape was least-squares fit to an empirical asymmetric Lorentzian. The same line shape, with a multiplicative prefactor, was then used to describe the combination of free surfactant and surfactant coating the nanotubes in the mixtures. The intensities, rather than amplitudes, of the nanotube and surfactant contributions were added; this is rigorously correct for the random mixture of nanotubes and pure surfactant and is a reasonable approximation for the surfactant coating the nanotubes, because the cross-terms are small over most of the Q range studied. Since the interesting part of the scattering profile for network structure is at lower Q, the details of the high Q data do not substantially affect the line shape at small Q. However, the uncertainty in the surfactant fraction is the biggest single contribution to the uncertainty in the crossover point. Even

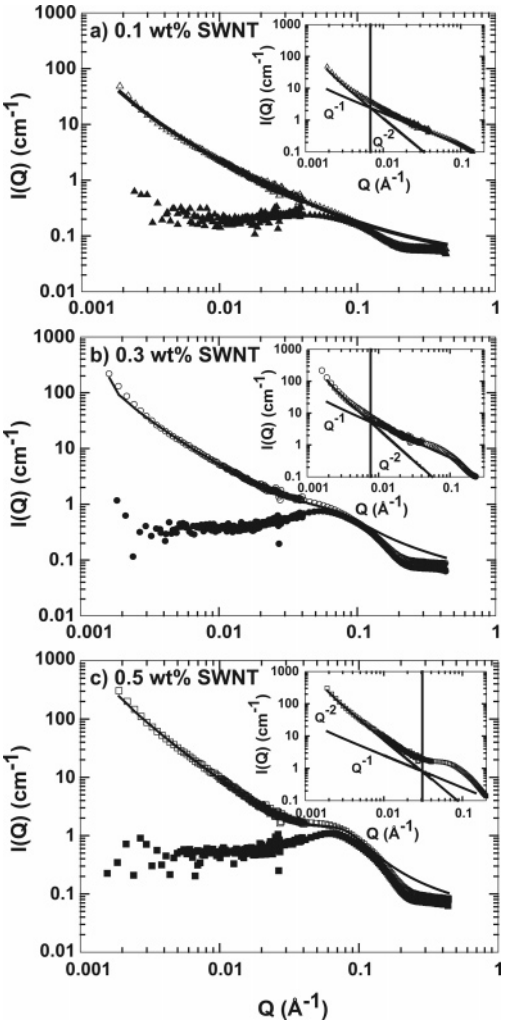

Figure 2. SANS scattering: SWNT + NaDDBS suspensions, open symbols; corresponding surfactant solution, closed symbols. The ratio of SWNT to NaDDBS was held fixed at 1:5. (a) Open triangles, 0.1 wt% SWNT. (b) Open circles, 0.3 wt% SWNT. (c) Open squares, 0.5 wt% SWNT. The solid line is a fit to the model described in the text. The inset of each figure shows the individual contributions from rigid rod Q^{-1} and network Q^{-2} structure, as well as the crossover between the two.

when incorporating the surfactant fraction, the data were described only moderately well at high Q by the assumed functional form. Therefore, fits were performed to the data only below $Q = 0.03$ Å^{-1}.

A second important consideration was the Q-dependent instrumental resolution, which had a substantial and qualitative effect on the scattered intensities, particularly at the smallest scattering angles. In particular, it was crucial to incorporate the instrumental resolution in the calculated line shape by convoluting the bare line shape with the instrumental resolution function. The Q-dependent instrumental resolution for the NIST SANS instrument is well understood.[32] The resolution was calculated and recorded by the data collection software for each data point and subsequently incorporated in the data analysis. The entire model therefore incorporated a dual power law line shape convoluted with the resolution function, a surfactant contribution with adjustable amplitude, and a constant incoherent contribution. The functional form of the model is given by

$$I = I_{\text{power}}(Q) + fI_{\text{surf}}(Q) + I_{\text{incoh}}$$

$$I_{\text{power}}(Q) = A \int R(Q - Q')G(Q')\,\mathrm{d}Q'$$

$$G(Q) = \begin{cases} Q^{-2} + Q_c^{-1}Q^{-1} & Q > 0 \\ 0 & Q \le 0 \end{cases}$$

Here, I_{incoh} is the incoherent scattering contribution, fixed at 0.04 for all data sets. The crossover from Q^{-1} to Q^{-2} is given by Q_c. f is a prefactor applied to the surfactant contribution and can be loosely interpreted as the fraction of surfactant that has not coated the surface. $G(Q)$ is the "bare" power law line shape. I_{power} is the power law contribution convoluted with the instrumental resolution (which varied with Q and was known for each data point). The numerical convolution of the power law line shape with a Gaussian resolution function was efficiently performed using 10-point Hermite integration, as previously described.[33] The solid lines in Figure 2 represent best fits to the data using eq 1.

The crossover from Q^{-1} to Q^{-2} behavior gives the mesh size or correlation length, ξ, of the network. At length scales smaller than the mesh size, see Figure 1c, the structure of the suspension is identical to a rigid rod (individual SWNTs). At length scales larger than the mesh size, the structure of the suspensions behaves like a network of randomly oriented rods. The same Q^{-2} behavior is observed in other random systems, such as dilute and semidilute solutions of polymers in a theta solvent, or branched polymers.[34] When we allowed the exponent for the small Q behavior to vary around the value of 2, we obtained exponents between 1.9 and 2.5. This uncertainty in the exponent implies that we cannot unambiguously distinguish between a percolating three-dimensional mesh (Q^{-2}) or a percolating diffusion-limited cluster model ($Q^{-2.5}$). The position of the crossover in Q from isolated rod behavior to network behavior, however, was not sensitive to the change in the exponent for the low Q behavior.[35,36]

Table 1 shows the fraction of surfactant scattering intensity used in the fits, and the Q_c determined by the fit. The mesh size was calculated from $\xi = 2\pi/Q_c$. At very large concentrations of SWNTs (>0.75 wt%), the crossover was obscured by the surfactant scattering, and we could not accurately

Table 1. Average Q_c and the Average Mesh Size As Determined from the SANS Intensity Profiles of Various Concentrations of SWNT Suspensions Stabilized by NaDDBS[a]

SWNT (wt %)	f	avg Q_c ($\times 10^{-3}$ Å^{-1})	avg ξ (nm)
0.1	0.0000	6.85	91.7
0.2	0.4020	7.33	85.7
0.3	0.4020	7.72	81.3
0.4	0.5720	15.3	41.0
0.5	0.8170	30.9	20.3
0.75	0.7410	>40	<15

[a] The parameters are described in the text.

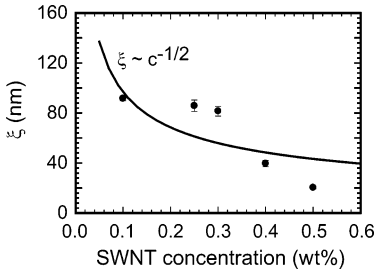

Figure 3. Dependence of the measured mesh size on SWNT concentration. The solid line indicates the variation of the mesh size with concentration based on theories for long semiflexible cylinders (rods) in the semidilute concentration regime.

determine ξ. The surfactant fraction f was a freely floating parameter in the fit, and the 50% uncertainty in the fitted value of f provided the single biggest contribution ($\sim$10%) to the uncertainty in Q_c. Nevertheless, the existence of a crossover point and the monotonic increase in Q_c with increasing SWNT concentration were both independent of f (whether it was fixed or allowed to vary). Figure 3 shows the dependence of the mesh size with increasing concentration. According to theory for long semiflexible cylinders in the semidilute concentration regime, the mesh size should vary according to $\xi \propto 1/\sqrt{c}$ where c is the concentration of rods (SWNTs).[25,26] Conversely, according to Shih et al., the mesh size of a fractal aggregate is $\xi \propto c^{1/(D_f-d)}$, where D_f is the fractal dimension and d is the spatial dimension. Since the low Q power law is the fractal dimension of the SWNT structure, according to this argument, we would expect for an aggregate with $D_f = 2$ that $\xi \propto c^{-1}$. For an aggregate with $D_f = 2.5$, we would expect[37] $\xi \propto c^{-2}$. Although the error bars are large, it appears the decrease in mesh size with increasing concentration is stronger than the predictions for a network of long semiflexible rods.

We next consider the effects of suspension quality on SANS profiles. Recent SANS studies from suspensions of SWNTs prepared with surfactants such as Triton X-100[18] and sodium dodecyl sulfate (SDS)[19] do not show rigid rod structure at any length scale, but rather show intensity variations reminiscent of a network structure at all accessible wave vectors (i.e., $\sim Q^{-2}$ over the entire accessible Q range). Wang et al. have suggested that the absence of rigid rod structure from these suspensions may be due to dispersion quality.[18] To test the effect of dispersion quality on the scattering profiles, we prepared a suspension of 0.08 wt% SWNT with a SWNT:NaDDBS ratio of 1:2 in D_2O.[38] This surfactant ratio (1:2) is insufficient to create a dispersion of isolated SWNTs.[11] Interestingly, the SANS profile for 0.08 wt% exhibits a $\sim Q^{-2}$ behavior over the entire Q range, as shown in Figure 4. This $\sim Q^{-2}$ behavior suggests the SWNTs do not behave like rigid rods over the length scales investigated by SANS. We suspect that insufficient surfactant concentrations prevents the formation of stable suspensions of isolated SWNTs. Instead, the suspension consists of bundles of SWNTs with a microscopic structure similar to that of isotropic aggregates. The aggregates might be self-similar to the SWNT networks, but because the mesh size would be much smaller (i.e., approximately the SWNT

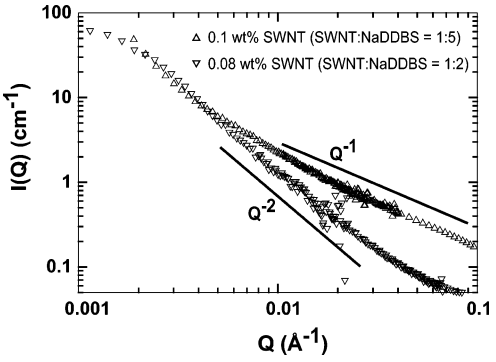

Figure 4. SANS intensity profiles for SWNT suspensions. The upright open triangles are the SANS intensity profile for 0.1 wt% SWNT (SWNT:NaDDBS = 1:5). The inverted open triangles are the SANS intensity profile for 0.08 wt% SWNT (SWNT:NaDDBS = 1:2). The solid line below the data is Q^{-2}, and the solid line above the data is Q^{-1}.

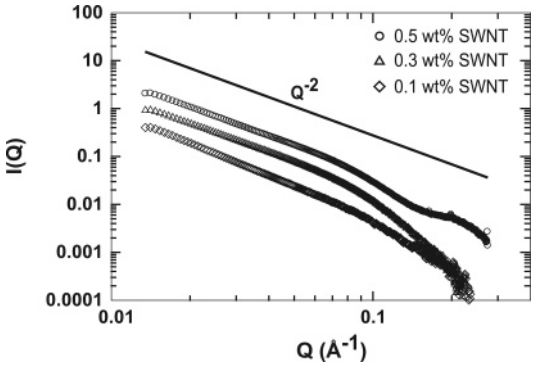

Figure 5. X-ray intensity profiles for various suspensions of SWNTs (SWNT:NaDDBS = 1:10): open circles, 0.5 wt% SWNT; upright open triangles, 0.3 wt% SWNT; open diamonds, 0.1 wt% SWNT. Intensities have been rescaled by arbitrary prefactors for clarity.

diameter of $\sim$1 nm), the $\sim Q^{-2}$ power law should extend to larger Q. Figure 4 also shows the SANS profile from a dispersion of 0.1 wt% SWNT with SWNT:NaDDBS ratio of 1:5. These data display the expected Q^{-1} dependence at large Q characteristic of a high-quality suspension of rigid rods.

X-ray diffraction is the other important scattering technique for probing microscopic structure on short length scales. X-ray scattering measurements of SWNT suspensions stabilized with sodium polystyrene sulfonate have not exhibited rigid rod behavior at any length scale.[15] To resolve the apparent discrepancy between X-ray and neutron diffraction measurements, we compared the two techniques using the same sample types. X-ray data were collected at the CMC−CAT beamline of the Advanced Photon Source, Argonne National Laboratory. SWNT suspensions were prepared at a surfactant ratio of 1:10 in water and loaded into glass capillaries with inner diameter of 1.5 mm. Figure 5 shows the X-ray scattering profiles of the suspensions after background subtraction. Although the surfactant ratio and the Q range are more than sufficient to observe Q^{-1}, the X-ray scattering profile exhibits a Q^{-2} behavior over the same range that SANS showed Q^{-1}.

The origin of the Q^{-2} behavior is uncertain. Nevertheless, no evidence exists for rigid rod structure in the X-ray measurements. One possible reason for this difference from SANS is a lack of X-ray scattering contrast between SWNTs and surfactant. Because SWNTs are coated with NaDDBS molecules, and because there are also NaDDBS molecules free in suspension, the contrast between the tubes and surfactant is important. We computed X-ray scattering length densities using a web-based scattering length density calculator provided by NIST.[39] The X-ray scattering length density (SLD) of the surfactant is calculated using the molecular formula ($CH_3(CH_2)_{11}C_6H_4SO_3Na$) and the density ($\rho \sim 1$ g/mL), $SLD_{X\text{-}ray}(NaDDBS) = 0.9 \times 10^{-5}$ Å^{-2}. The X-ray SLD of the SWNTs is similarly calculated. Assuming the density of a chiral nanotube to be ($\rho \sim 1.4$ g/mL), $SLD_{X\text{-}ray}(SWNT) = 1 \times 10^{-5}$ Å^{-2}. These scattering lengths are so close to one another that there is indeed very little contrast between SWNTs and surfactant. Thus, it is difficult to distinguish the nanotube scattering from the surfactant background with X-rays, at least for our samples. Note that the contrast should be similar for other alkane chain based surfactants (e.g., sodium dodecyl sulfate, Triton X-100, etc.). On the other hand, the neutron scattering SLD for SWNTs is calculated to be $SLD_{neutron}(SWNT) = 4.6 \times 10^{-6}$ Å^{-2} and has been measured[17] to be $SLD_{neutron\ measured}(SWNT) = 4 \times 10^{-6}$ Å^{-2}, more than five times larger than the calculated SLD for NaDDBS $SLD_{neutron}(NaDDBS) = 0.6 \times 10^{-6}$ Å^{-2}. Therefore, SANS should be the preferred technique for measuring surfactant-stabilized SWNT suspensions.

In conclusion, we measured SANS intensity profiles for NaDDBS stabilized SWNT suspensions as a function of SWNT concentration in the *semidilute* regime. Rigid rod behavior was observed at large Q and a crossover to network behavior was also observed in these stable nanotube suspensions and gels. The crossover from rigid rod to network behavior provided the mesh size of each network, and the mesh size was found to decrease with increasing SWNT concentration. Inadequately dispersed SWNTs, for example at low SWNT-surfactant ratios, did not exhibit rigid rod behavior in the SANS profiles. In addition, X-ray measurements on the same stable NaDDBS-stabilized SWNT suspensions and contrast calculations suggest X-ray scattering is limited as a probe of these systems as a result of the poor contrast between SWNTs and NaDDBS.

Acknowledgment. We thank D. M. Casa and M. Bryning for their assistance with the X-ray measurements. We are also grateful to E. Hobbie and B. Bauer for enabling us to collect SANS data for SWNT suspensions of 0.08 wt% at NIST. This work was supported by the NSF (DMR 05-20020 (MRSEC) (A.G.Y., P.A.H.), DMR-0505048 (A.G.Y.), DMR-0102459 (P.A.H.), DMR-9986442 (B.H.)) and was partially supported by NASA, Grant NAG8-2172 (A.G.Y.). The Advanced Photon Source is supported by the U.S. Department of Energy under Contract No. W-31-109-ENG-38. The identification of any commercial product or trade name does not imply endorsement or recommendation by the National Institute of Standards and Technology.

References

(1) Baughman, R. H.; Zakhidov, A. A.; de Heer, W. A. *Science* **2002**, *297*, 787.
(2) de Heer, W. A.; Bacsa, W. S.; Chatelain, A.; Garfin, T.; Humphrey-Baker, R.; Forro, L.; Ugarte, D. *Science* **1995**, *268*, 845.
(3) Odom, T. W.; Huang, J. L.; Kim, P.; Lieber, C. M. *Nature* **1998**, *391*, 62.
(4) Dekker, C. *Phys. Today* **1999**, *52*, 22.
(5) Kong, J.; Franklin, N.; Zhou, C.; Chapline, M.; Peng, S.; Cho, K.; Dai, H. *Science* **2000**, *287*, 622.
(6) Wu, Z.; et al. *Science* **2004**, *305*, 1273.
(7) Ericson, L. M.; et al. *Science* **2004**, *305*, 1447.
(8) Bryning, M.; Islam, M. F.; Kikkawa, J. M.; Yodh, A. G. *Adv. Mater.* **2005**, *17*, 1186.
(9) Bryning, M. B.; Milkie, D. E.; Islam, M. F.; Kikkawa, J. M.; Yodh, A. G. *Applied Phys. Lett.* **2005**, *87*, 161909.
(10) Treacy, M. M. J.; Ebbesen, T. W.; Gibson, J. M. *Nature* **1996**, *381*, 678.
(11) Islam, M. F.; Rojas, E.; Bergey, D. M.; Johnson, A. T.; Yodh, A. G. *Nano Lett.* **2003**, *3*, 269.
(12) Hough, L. A.; Islam, M. F.; Janmey, P. A.; Yodh, A. G. *Phys. Rev. Lett.* **2004**, *93*, 168102.
(13) MacKintosh, F. C.; Kas, J.; Janmey, P. A. *Phys. Rev. Lett.* **1995**, *75*, 4425.
(14) Storm, C.; Pastore, J. J.; MacKintosh, F. C.; Lubensky, T. C.; Janmey, P. A. *Nature* **2005**, *435*, 191.
(15) Schaefer, D. W.; Zhao, J.; Brown, J. M.; Anderson, D. P.; Tomlin, D. W. *Chem. Phys. Lett.* **2003**, *375*, 369.
(16) Schaefer, D. W.; Brown, J. M.; Anderson, D. P.; Zhao, J.; Chokalingam, K.; Tomlin, D. W.; Ilavsky, J. *J. Appl. Crystallogr.* **2003**, *36*, 553.
(17) Zhou, W.; Islam, M. F.; Wang, H.; Ho, D. L.; Yodh, A. G.; Winey, K. I.; Fischer, J. E. *Chem. Phys. Lett.* **2004**, *384*, 185.
(18) Wang, H.; Zhou, W.; Ho, D. L.; Winey, K. I.; Fischer, J. E.; Glinka, C. J.; Hobbie, E. K. *Nano Lett.* **2004**, *4*, 1789.
(19) Yurekli, K.; Mitchell, C. A.; Krishnamoorti, R. *J. Am. Chem. Soc.* **2004**, *126*, 9902.
(20) Hobbie, E. K. *J. Chem. Phys.* **2004**, *121*, 1029.
(21) Dror, Y.; Pyckhout-Hintzen, W.; Cohen, Y. *Macromolecules* **2005**, *38*, 7828.
(22) Moore, V. C.; Strano, M. S.; Haroz, E. H.; Hauge, R. H.; Smalley, R. E. *Nano Lett.* **2003**, *3*, 1379.
(23) Vigolo, B.; Coulon, C.; Maugey, M.; Zakri, C.; Poulin, P. *Science* **2005**, *309*, 920.
(24) Schurtenberger, P.; Magid, L. J.; King S. M.; Lindner, P. *J. Phys. Chem.* **1991**, *95*, 4173.
(25) deGennes P.; Pincus, P.; Velasco R. M.; Brochard F. *J. Phys. II* **1976**, *37*, 1461.
(26) Schmidt, C. F.; Barmann, M.; Isenberg, G.; Sackmann, E. *Macromolecules* **1989**, *22*, 3638.
(27) Islam, M. F.; Milkie, D. E.; Kane, C. L.; Yodh, A. G.; Kikkawa, J. M. *Phys. Rev. Lett.* **2004**, *93*, 037404.
(28) Islam, M. F.; Milkie, D. E.; Torrens, O. N.; Yodh, A. G.; Kikkawa, J. M. *Phys. Rev. B Rapid Commun.* **2005**, *71*, 201401(R).
(29) Richard, C.; Balavoine, F.; Schultz, P.; Ebbesen, T. W.; Mioskowski, C. *Science* **2003**, *300*, 775.
(30) Kawasaki, H.; Ban, K.; Maeda, H. *J. Phys. Chem. B* **2004**, *108*, 16746.
(31) Nielsen, S. O.; Srinivas, G.; Lopez, C. F.; Klein, M. L. *Phys. Rev. Lett.* **2005**, *94*, 228301.
(32) Barker, J.; Pedersen, J. S. *J. Appl. Crystallogr.* **1995**, *28*, 105.
(33) Heiney, P. A.; Butera, R. J.; Londono, J. D.; Davidson, R. V.; Mazur, S. *J. Phys. Chem. B* **2000**, *104*, 8807.
(34) Jannink, G.; Des Cloizeaux, J. *Polymers in Solution*; Oxford University Press: Oxford, 1992.
(35) Beaucage, G. *J. Appl. Crystallogr.* **1996**, *29*, 134.
(36) Mohraz, A.; Moler, D. B.; Ziff, R. M.; Solomon, M. J. *Phys. Rev. Lett.* **2004**, *92*, 155503.
(37) Shih, W.-H.; Shih, W. Y.; Kim, S.-I.; Liu, J.; Aksay, I. A. *Phys. Rev. A* **1990**, *42*, 4772.
(38) Data for 0.08 wt % SWNT were collected using the 13 m NG7 line at NIST.
(39) http://www.ncnr.nist.gov/resources/sldcalc.html.

NL051871F